International Journal of Nanoelectronics and Materials
IJNeaM
ISSN 198-5761 | E-ISSN 2232-1535

Aluminium Interdigitated Electrode with 5.0 µm Gap for Electrolytic Scooting

M. N. Afnan Uda[a,*], Uda Hashim[a,b], M. N. A. Uda[b,c,e], Tijjani Adam[d], Asral Bahari Jambek[d], Ismail Saad[a], N. A. Parmin[b], Shahidah Arina Shamsuddine[e], N. A Karime[e], G. Yashni[f], Nur Hulwani Ibrahim[b], N. Parimon[a], and M. F. H. Rani[g]

[a]*Faculty of Engineering, Universiti Malaysia Sabah, 88400 Kota Kinabalu, Sabah, Malaysia.*
[b]*Institute of Nano Electronic Engineering, Universiti Malaysia Perlis, 01000 Kangar, Perlis, Malaysia.*
[c]*Centre of Excellence for Biomass Utilization, Universiti Malaysia Perlis, 02600 Arau, Perlis, Malaysia.*
[d]*Faculty of Electronic Engineering & Technology, Universiti Malaysia Perlis, Kampus Tetap Pauh Putra, 02600, Arau, Perlis, Malaysia.*
[e]*Faculty of Mechanical Engineering & Technology, Universiti Malaysia Perlis, Kampus Tetap Pauh Putra, 02600 Arau, Perlis, Malaysia.*
[f]*Faculty of Engineering & Computer Technology (FECT), AIMST University, 08100 Bedong-Semeling, Kedah, Malaysia.*
[g]*Institute for Vehicle Systems and Engineering (IVeSE), Universiti Teknologi Malaysia, 81310 Johor Bahru, Johor, Malaysia.*
**Corresponding author. Tel.: +60-194728844; e-mail: nurafnan@ums.edu.my*

ABSTRACT

The goal of the research project is to design, fabricate, and characterize an extremely sensitive biosensor for use in healthcare. Using AutoCAD software, a novel IDE pattern with a 5 µm finger gap was created. Conventional photolithography and regular CMOS technology were used in the fabrication process. A 3D nano profiler, scanning electron microscopy (SEM), high-power microscopy (HPM), and low-power microscopy (LPM) were used to physically characterize the manufactured IDE. Chemical testing was done using several pH buffer solutions, and electrical validation was performed using I-V measurements. The Al IDE was produced, with a tolerance of 0.1 µm between the fabricated IDEs and the design mask. Electrical measurements verified the flawless fabrication of the IDE, and the device's repeatability was validated by the outcomes of comparable IDE samples. For each pH buffer solution, a modest additional volume of 2 µl was used to quantitatively detect slight current fluctuations in the microampere range. Through pH calibration for advanced applications in the realm of chemical sensors using an amperometric method, this research study has verified the chemical behavior of the IDE.

Keywords: *Aluminium, Amperometric, Biosensor, Interdigitated Electrode, Surface chemistry*

1. INTRODUCTION

Today's point-of-care biosensors in healthcare facilities and environmental security rely on extremely sensitive sensors capable of detecting low quantities of bacteria within a sample [1], [2]. To detect and characterize bioatoms, ultra-miniaturized sensors have been developed using nanotechnology and smaller manufacturing scales [3], [4]. The interaction of microscale electrode fingers, typically arranged in an alternating pattern, is central to the concept of Interdigitated Electrodes (IDEs) [5]–[7]. By optimizing the electrode surface area within a confined space, this configuration can enhance analyte-electrode interactions and consequently improve sensor performance. Due to its excellent electrical conductivity, lightweight nature, and cost-effectiveness, aluminum is a popular material for fabricating IDEs [8], [9]. The demands for small-scale nanogap biosensors include sensitivity, simplicity, user-friendliness, reliability, speed, affordability, adaptability, and multi-analyte detection capabilities [10]–[12].

The fields of medicine, genetic research, agriculture, the military, drug discovery, assessment of nutritional damage, and industrial process monitoring represent promising application areas for small-scale nanogap biosensors. Strategically, a 5.0 µm interdigitated gap was selected to strike a balance between analyte diffusion kinetics and electrode spacing [13]–[15]. This optimization of gap size facilitates efficient transport of target analytes to the electrode surface, leading to rapid response times and maintained sensitivity. Attaining the desired sensing characteristics for a specific application necessitates precise control over electrode design. Due to the relatively straightforward estimation and construction of downsized sensors, amperometric-based detection emerges as a viable electrochemical sensor technology [16]–[18]. Furthermore, the sensor based on the interdigitated electrode design offers several advantages and areas of interest in biosensor development due to its fundamental architecture. These sensors play a crucial role in the system's responses, either through the generation or utilization of charged species [19], [20].

In several domains, such as industrial process control, biological diagnostics, and environmental monitoring, electrochemical sensing has become an indispensable instrument [21]–[23]. Interdigitated electrodes (IDEs), one of the many types of electrodes used in electrochemical sensing, have attracted a lot of interest because of its low cost, high sensitivity, and ability to be miniaturised. This introduction explores the novel field of aluminium interdigitated electrodes (Al IDEs) designed for electrolytic scouting applications, with a gap size of 5.0 µm [24], [25].

It modifies the current flowing through the test material's ionic composition when it is positioned between the electrodes [26]–[29].

Since aluminium (Al) has a better conductive structure and is less expensive than other highly conducting materials like au, pt, and cu, it was used as the electrode material [30]–[32]. Taking a closer look at Al IDEs with a 5.0 μm gap for electrolytic reconnaissance, this introduction lays the groundwork for deciphering the fundamental ideas, practical issues, and future uses of these novel electrodes [33]–[35]. Clarifying the revolutionary influence of this state-of-the-art sensing platform on electrolytic scouting techniques through methodical research and empirical confirmation, opens new avenues for analytical science and other fields [36]–[38]. The development of ultra-sensitive biosensing and detection tools using Al has received a great deal of attention in recent years. Additionally, outstanding efforts in the field of nanotechnology advancement are thought to be promising tools for improving several sectors for better applications.

The primary goal of the study is to design, fabricate, and characterize an inexpensive IDE for use in biosensor applications. AutoCAD software is used to design the photomask. Conventional photolithography and regular CMOS technology are employed in the fabrication process. Silicon (Si) serves as the substrate, with Aluminum (Al) used as the conducting material. Once the fabrication process is completed, the Al IDE undergoes physical testing using high-power microscopy (HPM), low-power microscopy (LPM), scanning electron microscopy (SEM), and 3D nano profiler. Electrical characterization is performed using I-V measurements, while chemical testing is conducted using pH buffer solutions, including alkali and hydroxyl solutions.

2. MATERIAL AND METHODS

2.1. Chemical and Reagents

All of the substances used in this investigation were of analytical reagent grade to ensure the highest degree of purity and consistency in the outcomes of the experiments. The principal suppliers of necessary materials and chemicals for the fabrication process and experimental techniques were Mallinckrodt Baker and Futurrex, Inc. Several essential components were provided by Mallinckrodt Baker, including the silicon wafer substrate, acetone, sodium hydroxide (NaOH), and various cleaning solutions such as RCA1 and RCA2. They also supplied chemicals like hydrogen peroxide, hydrogen fluoride, ammonium hydroxide, and hydrochloric acid for surface modification and cleaning. Using a 10-micropipette, two milliliters of different pH buffer solutions were deposited onto the active surface of the IDEs as part of the experimental procedures. This allowed for precise management and uniform distribution of the buffer solutions in preparation for further electrochemical characterization and analysis. This study aimed to ensure the consistency and accuracy of experimental results by utilizing high-quality chemicals and standardized techniques, thereby establishing a solid foundation for reliable data interpretation and scientific advancement in the field of electrochemical sensing and characterization. Futurrex, Inc. supplied the positive photoresist (PR1-2000A) and resist developer (RD6), which are essential for lithographic patterning procedures, to the experimental setup. To ensure consistent quality and purity, ethanol and deionized distilled water (DDI-water) were procured from Sigma Aldrich in the US. Analytical-grade buffer solutions with pH values of 3, 7, 10, and 12 were utilized for chemical characterization and calibration. These buffer solutions served as reference standards for evaluating the electrochemical behavior of the interdigitated electrodes (IDEs) and for pH measurements.

2.2. Instruments

The surface morphology and structural analysis of the aluminum interdigitated electrode (Al IDE) pattern were meticulously conducted using a combination of sophisticated microscopy methods and precise characterization instruments. Various microscopy tools were employed to analyze the surface morphology, including high-power microscopy (HPM) and low-power microscopy (LPM), which provided comprehensive insights into the characteristics of the Al IDE pattern's surface. The JEOL JSM-610LV scanning electron microscope, operating at 20 kV with a magnification of 7000x, enabled high-resolution imaging of the electrode structure at room temperature, revealing minute features and structural subtleties crucial for understanding the surface properties of the electrode. Additionally, to investigate the three-dimensional (3D) features of the electrode morphology and enhance the analysis, a surface 3D profilometer—specifically, the Hawk 3D nano-profiler—was utilized. With a magnification of 50,000x, this device provided accurate topographical data, facilitating a comprehensive study of grain structures between IDE finger electrodes. In addition to morphological study, electrical characterization was conducted to evaluate the functionality and performance of the Al IDE pattern. This involved the use of a voltage source, namely the Keithley 2450, a probe station, and Kickstart software for current-voltage (I-V) characterization measurements. By determining important electrical parameters such as resistance and current-voltage curves, these tests illuminated the electrochemical behavior and functionality of the Al IDE pattern under various operating conditions. Through a synergistic approach that combined sophisticated microscopy techniques with precise characterization tools, this comprehensive characterization project aimed to elucidate the complex interplay among the Al IDE pattern's surface morphology, structural features, and electrical properties. The optimization of device performance, advancement of understanding of electrochemical processes, and promotion of innovation in the field of microscale electrode design and fabrication all hinge on such thorough investigation.

2.3. Design of the Interdigitated Electrode (IDE)

Using AutoCAD software, the photomask for the IDE biosensor was created and printed onto a chrome glass surface. For the photomask procedure, a standard chrome mask was employed. Figure 1 and Table 1 present a tabulation of the updated Al IDE specifications.

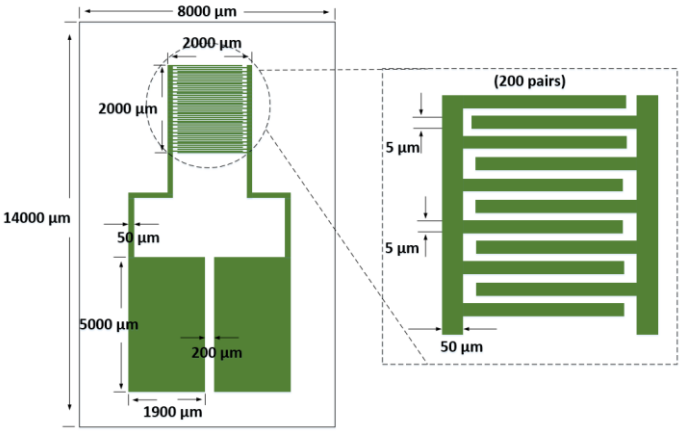

Figure 1. A new pattern of the Aluminium Interdigitated Electrode photomask to design using AutoCAD software.

Table 1 The new pattern of the Aluminium Interdigitated Electrode design dimension

Description	Value (µm)
The size of the gap	5
The width of the finger	5
The length of the finger	5
The size of the electrode	50
The size of the contact area	2000
The width between electrode	2000
Pad size	5000 x 1900
Number of devices	400 (200 pairs)
Device area	2000 x 2000
Total Size	14000 x 8000

2.4. Fabrication of Aluminium Interdigitated Electrode

The entire Al IDE biosensor production process flow is depicted in Figure 2. The basic material was P-type Si substrate. wafer, which was conducted for 45 minutes at 750 ˚C. Next, use the sputtering technique to deposit the Al layer on top of the SiO2 surface. The patterning process involved the deposition of an Al layer using the photolithography method. In this technique, the spin coating process was used to cover a positive photoresist on the Al surface. After that, the SiO2 substrate was soft-baked for two minutes at 80 ˚C to remove any remaining moisture and the standing wave on the positive PR layer.

The IDE mask was positioned, and it was covered with UV light for 15 seconds to transfer the mask onto the sample's surface. As the last stage of photolithography, advancement preparation lasted for 30 seconds, followed by a hard bake at 130 ˚C for 2 minutes to drive out excess moisture and strengthen the adhesive force between the Al and SiO2 layer. Afterwards, the exposed area was removed by submerging it in Al etch for 20 seconds. Finally, the photoresist was removed from the test by using acetone to clean it. Figure 3 shows the Al IDE that was created by a basic photolithography method.

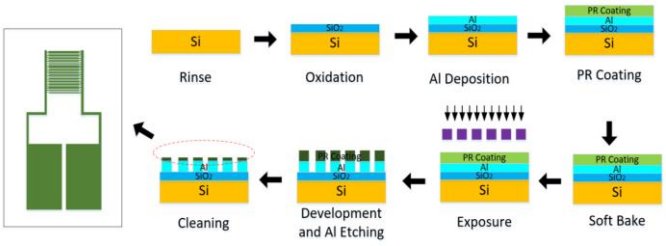

Figure 2. The complete fabrication process flow of the Aluminium Interdigitated Electrode.

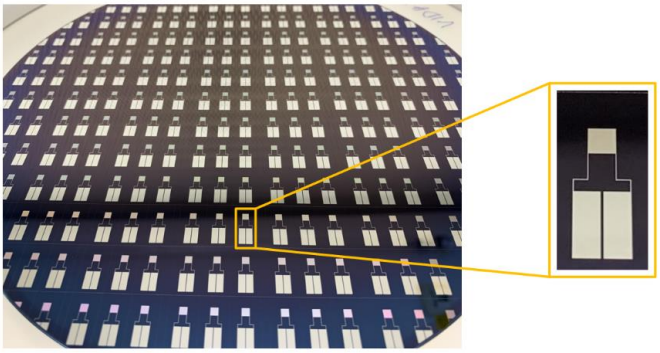

Figure 3. Ready-made of Fabricated Aluminium Interdigitated Electrode (IDE) using the Photolithography Process.

3. RESULTS AND DISCUSSION

Al IDE was intended to be an electrochemical sensor with characterization and preparation were necessary before proceeding with pH-based chemical investigation. To ensure that the estimation remains unaffected during the I-V characterization method, it is important to establish without a doubt that the creation handle is done cautiously. To identify the Al IDE surface's layout, the well-fabricated surface was advanced characterized by LPM, HPM, SEM, and 3D nano-profiler.

3.1. Measurement of Surface Morphology

In each example, Figure 4a–b were viewed at multiple magnifications, 3.5x and 7.5x LPM. There are a tonne of IDE fingers in the active surface region, as seen in Figure 4a. Figures 4c and d show the IDE electrode finger patterns from HPM at 30x and 50x magnifications, respectively. Al finger electrodes, as seen in Figures 4c and d, are produced with exact measurements for the electrode finger distance from the electrode, electrode finger gap, and electrode finger width 5, 5 and 50 µm, respectively. Verify that the LPM and HPM images show a uniform structure with no shortage or imperfections on the surface, and that the entire IDE is neatly built in accordance with the intended dimensions.

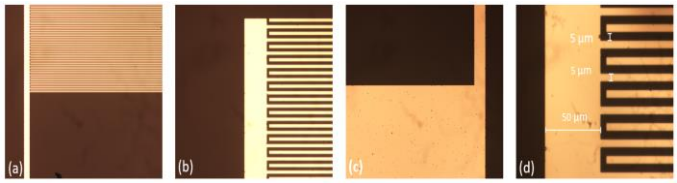

Figure 4. The LPM and HPM images of the Al IDE electrode. a) LPM image is magnified 3.5 times; b) the LPM image is magnified 7.5 times; c) the HPM image is magnified 30 times; d) the HPM image is magnified 50 times at room temperature.

3.2. Scanning Electron Microscope (SEM) Images

The SEM picture of the finger electrodes in the constructed Al IDE's active surface area on the Si substrate is displayed in Figure 5. The fingers in IDEs seemed to be well-made at the microscale, with somewhat smooth and sharp edges. The graphic indicates that the finger width, spacing between electrodes, and distance between electrode fingers are 4.93, 4.96, and 49.2 µm, respectively. The SEM scans verified that the Al IDE sensor's fingers have crisp edges, that there are no shortages in the fabrication process, and that the IDE's tolerance is almost 0.1 µm.

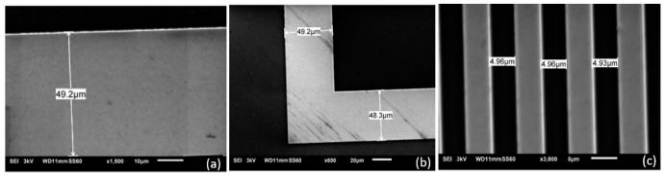

Figure 5. SEM image of the Al IDE distance from electrode fingers to the electrode, finger width, and gap between electrode fingers.

3.3. 3D Profiler Images

The study of the Al IDE structure using the 3D profiler is shown in Figure 6a. It shows some tightly spaced electrode fingers, which may further suggest that the etching has reached the highest point of the development phase. The variation in IDE height from bottom to top is indicated by different colours. The possibility for real-time measurement was demonstrated by the perpendicular resolution of the 3D mapping data. The Al surface's minimum height from the base level of the grain, as shown in Figure 6b, is 402.986 nm; its highest height is 409.315 nm and its average height is 406.445 nm. The finger IDE gap was displayed in Figure 6c, and it is verified that the finger IDE is expertly built from top to bottom. The spacing between the electrode fingers and the electrode is 53.0 µm, as seen in Figures 6d and 6e.

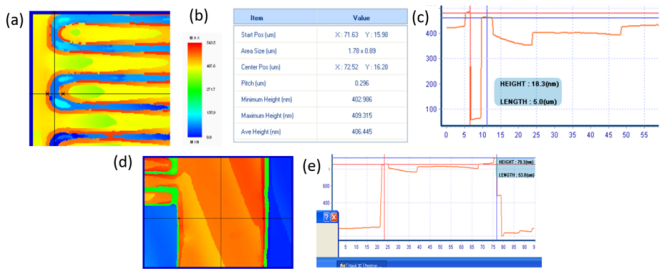

Figure 6. Al IDE, a 3D nano profiler, a) a 2D view; b) a specification table; c) a surface gap graph based on the finger gap indicated by the black line in the 2D picture; d) a 2D view of the distance between the electrode fingers and the electrode; and e) a surface gap graph for that distance.

3.4. Electrical Characterization

The electrical characterisation of the structure of Al IDEs is proposed in this research study. To ensure accuracy, electrical characterisation is carried out using current-voltage measurements utilising a pico ammeter-voltage source, namely the Keithley 2450. The current voltage (I-V) characteristics were obtained using the kick-start programme, a probe station, and the pico ammeter Keithley 2450, as shown in Figure 7. For the I-V characterization, the voltage between the two electrodes was swept between 0 and 1 V. After reaching a value of 0.5 V, the IDE device remained stable, nevertheless, going over this voltage range could be dangerous for the device. Five Al IDE devices were used for the electrical characterisation in order to guarantee dependability. The I-V characteristics of the bare Al IDEs are shown in Figure 8, and the results were constant over the whole voltage range that was examined. As seen in the graph, the current values at 1 V for five distinct bare Al IDEs were recorded as 23.3 pA, 23.1 pA, 23.9 pA, 23.6 pA, and 23.4 pA. The average current was found to be 23.5 pA, with only 0.8 pA separating the least and greatest current readings. The small range of current values indicates that there were no appreciable variations in the dimensions or characteristics of the IDEs throughout fabrication and processing.

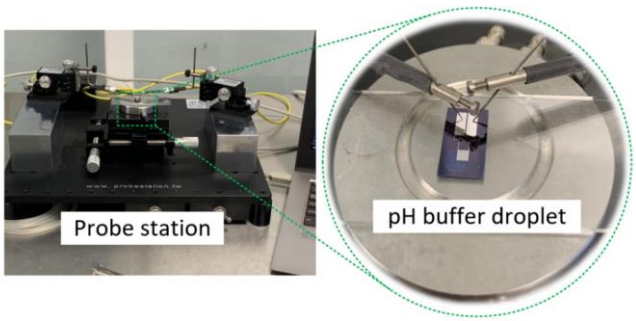

Figure 7. Electrical Characterization by using picoammeter Keithley 2450, Kick start software, and probe station.

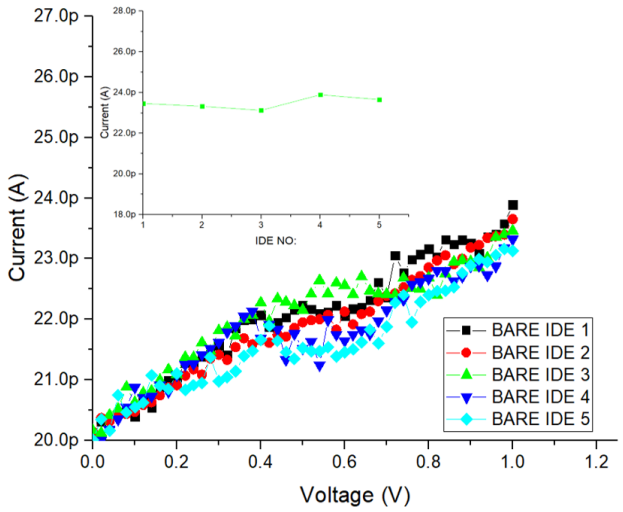

Figure 8. I-V characteristics on bare Aluminium Interdigitated Electrode.

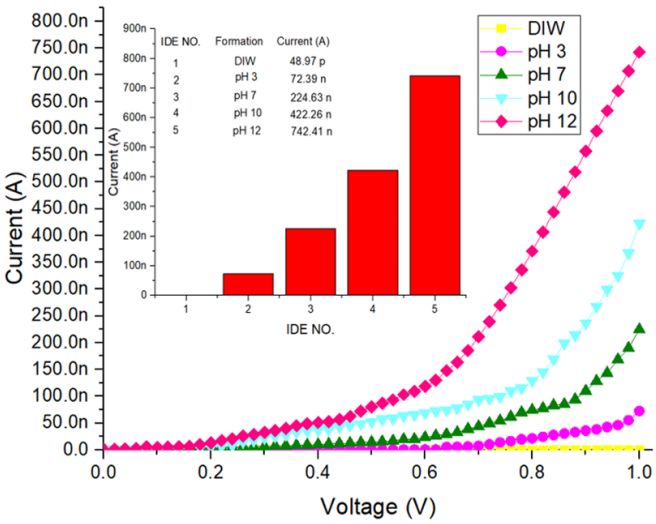

Figure 9. I-V measurements of the Aluminium Interdigitated Electrode with different pH measurements.

3.5. Chemical Characterization

In order to assess the chemical reaction of the accurately constructed Al IDEs, two millilitres (µL) of different pH buffer solutions were gradually applied to the Al IDE device's active surface area while it was at room temperature. For this chemical analysis, commercially available pH buffer solutions were utilised, more especially pH 3, pH 7, pH 10, and pH 12 from QREC. Figure 7 shows how the Keithley 2450, probe station, and kick-start software were used to record the Al IDE device's reaction to these buffer solutions. I-V measurements were carried out with the same Al IDE at various pH values. Starting at pH 3, the most acidic solution was measured, then pH 7, pH 10, and pH 12, which was the most alkaline level. Each buffer solution was applied, and the current was measured after an incubation time of five minutes. The I-V readings of the Al IDE sensor for pH values 3, 7, 10, and 12 are shown in Figure 9. As demonstrated in Figure 9, the data show a distinct trend when the pH rises from 3 to 12, current rises in tandem. The current data showed the following pattern, specifically, at 1 V. The measurements for DIW were 48.97 pA, pH 3; pH 7, pH 10, pH 11, and pH 12, 72.39 nA, 224.63 nA, and 742.41 nA, respectively.

The existence and actions of ions in the solution are frequently responsible for the phenomenon of current rise in electrolytic systems. Specifically, hydroxide ion concentration (OH^-) is a major factor in regulating electrical conductivity and, in turn, current flow, particularly under alkaline circumstances. The abundance of hydroxide ions is noticeably higher at pH values of 10 and 12. At these pH levels, the extremely alkaline surroundings encourage the dissociation of water molecules, which raises the hydroxide ion concentration. This excess of OH^- ions greatly increases the solution's ionic conductivity, which speeds up the transport of charged species and raises the electrolytic system's current flow. The increased hydroxide ion concentration affects the electrode processes at the interface in addition to increasing ionic conductivity. Hydroxide ions have the ability to take part in a variety of redox processes in electrochemical systems, which can impact the kinetics of electron transfer and eventually alter the measured current. All things considered, the high concentration of hydroxide ions, which improve ionic conductivity and regulate the electrode processes inside the electrolytic system, is responsible for the noticeable rise in current that was recorded at pH 10 and pH 12. The comprehension of the relationship among pH, ion concentration, and current response is imperative in the enhancement of electrolytic processes and the development of effective electrochemical sensing platforms. Thus, Analyte identification and quantification in complicated matrices using electrochemical techniques is the focus of the emerging discipline of electrolytic scouting. Electrolytic scouting shows great promise for improving analytical capabilities, whether it is used for real-time biological fluid analysis or the monitoring of trace pollutants in environmental samples.

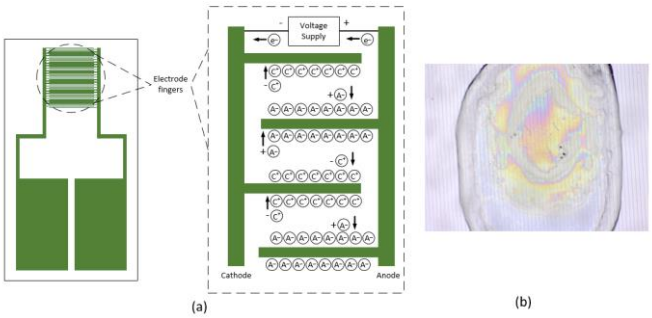

Figure 10. Mechanism of electrolysis charges for the i(a) ion transfer and pH detection by Aluminium Interdigitated Electrode.

4. CONCLUSION

This study uses CMOS technology and conventional lithography to achieve a new pattern Using LPM, HPM, well-fabricated IDE was effectively physically observed. Here, the use of Al IDEs with an interdigitated gap of 5.0 µm is a noteworthy development that provides improved electrolytic scouting endeavours in terms of sensitivity, selectivity, and reliability. These IDEs are a strong competitor in the field of electrochemical sensing because of the intrinsic qualities of aluminium and the carefully designed electrode architecture., Kickstart programme, and voltage source Keithley 2450. Electrical characteristics on the unadorned Al IDE verified that the gadget is well-built, devoid of flaws. The Al IDE sensor's sensitivity for various pH ranges has been determined by the acquired pH data. The sensitivity of IDEs in both acidic and alkaline solutions has been confirmed. The higher sensitivity of the suggested IDE with a 5 µm design makes it promising for a range of biosensor applications. Its small size and interdigitated structure provide increased surface area, making it suitable for detecting biomolecules like glucose, DNA, and proteins. Additionally, its compatibility with both acidic and alkaline environments extends its applicability across diverse fields, encompassing healthcare, environmental monitoring, and industrial processes.

ACKNOWLEDGMENTS

The author would like to thank all staff members of the Institute of Nanoelectronic Engineering in Universiti Malaysia Perlis (UniMAP) for their technical advice and contributions, directly and indirectly.

REFERENCES

[1] Y. Song, Y. Luo, C. Zhu, H. Li, D. Du, and Y. Lin, "Recent advances in electrochemical biosensors based on graphene two-dimensional nanomaterials," *Biosens. Bioelectron.*, vol. 76, pp. 195–212, 2016, doi: 10.1016/j.bios.2015.07.002.

[2] T. Mocan *et al.*, "Development of nanoparticle-based optical sensors for pathogenic bacterial detection," *J. Nanobiotechnology*, vol. 15, no. 1, pp. 1–14, 2017, doi: 10.1186/s12951-017-0260-y.

[3] M. Nur *et al.*, "Conductometric immunosensor for specific Escherichia coli O157 : H7 detection on chemically funcationalizaed interdigitated aptasensor," *Heliyon*, vol. 10, no. 5, p. e26988, 2024, doi: 10.1016/j.heliyon.2024.e26988.

[4] N. A. Parmin, U. Hashim, N. Hamidah A Halim, M. N. A. Uda, and M. N. Afnan Uda, "Characterization of Genome Sequence 2019 Novel Coronavirus (2019-nCoV) by using BioinformaticTool," *IOP Conf. Ser. Mater. Sci. Eng.*, vol. 864, no. 1, p. 012168, 2020, doi: 10.1088/1757-899X/864/1/012168.

[5] T. B. Tran, S. J. Son, and J. Min, "Nanomaterials in label-free impedimetric biosensor: Current process and future perspectives," *Biochip J.*, vol. 10, no. 4, pp. 318–330, 2016, doi: 10.1007/s13206-016-0408-0.

[6] S. Nadzirah, N. Azizah, U. Hashim, S. C. B. Gopinath, and M. Kashif, "Titanium dioxide nanoparticle-based interdigitated electrodes: A novel current to voltage DNA biosensor recognizes E. coli O157:H7," *PLoS One*, vol. 10, no. 10, pp. 1–15, 2015, doi: 10.1371/journal.pone.0139766.

[7] S. Arora, N. Ahmed, and S. Siddiqui, "Detecting food borne pathogens using electrochemical biosensors : An overview," *Int. J. Chem. Stud.*, vol. 6, no. 1, pp. 1031–1039, 2018.

[8] J. G. Bruno, "Fluorescent DNA Aptamer-Magnetic Bead Sandwich Assays and Portable Fluorometer for Sensitive and Rapid Foodborne Pathogen Detection and Epidemiology," *J. Infect. Dis. Epidemiol.*, vol. 2, no. 1, pp. 2–7, 2016, doi: 10.23937/2474-3658/1510011.

[9] V. K. Nigam and P. Shukla, "Enzyme based biosensors for detection of environmental pollutants-A review," *J. Microbiol. Biotechnol.*, vol. 25, no. 11, pp. 1773–1781, 2015, doi: 10.4014/jmb.1504.04010.

[10] T. Balasubramaniam *et al.*, "Potential of Syntesized Silica Nanoparticles (Si-NPs) using Corn Cob for Arsenic Heavy Metal Removal," *IOP Conf. Ser. Mater. Sci. Eng.*, vol. 864, no. 1, 2020, doi: 10.1088/1757-899X/864/1/012187.

[11] M. N. A. Uda, S. C. B. Gopinath, U. Hashim, and M. N. A. Uda, "Simple and Green Approach Strategy to Synthesis Graphene Using Rice Simple and Green Approach Strategy to Synthesis Graphene," *IOP Conf. Ser. Mater. Sci. Eng.*, vol. 1, 2020, doi: 10.1088/1757-899X/864/1/012181.

[12] M. N. Afnan Uda, A. B. Jambek, U. Hashim, and M. N. A. Uda, "Electrical DNA Biosensor Using Aluminium Interdigitated Electrode for Salmonella Detection," *IOP Conf. Ser. Mater. Sci. Eng.*, vol. 743, no. 1, 2020, doi: 10.1088/1757-899X/743/1/012022.

[13] M. N. Afnan Uda *et al.*, "Nano-micro-mili Current to Mili Voltage Amplifier for Amperometric Electrical Biosensors," *IOP Conf. Ser. Mater. Sci. Eng.*, vol. 743, no. 1, 2020, doi: 10.1088/1757-899X/743/1/012021.

[14] M. N. Afnan Uda, A. B. Jambek, U. Hashim, M. N. A. Uda, and M. A. F. Bahrin, "Aluminium Interdigitated Electrode Based Biosensor for Specific ssDNA Target Listeria Detection," *IOP Conf. Ser. Mater. Sci. Eng.*, vol. 743, no. 1, 2020, doi: 10.1088/1757-899X/743/1/012032.

[15] R. D. A. A. Rajapaksha, N. A. N. Azman, M. N. A. Uda, U. Hashim, S. C. B. Gopinath, and C. A. N. Fernando, "Multichannel PDMS microfluidic based nano-biolab-on-a-chip for medical diagnostics," *AIP Conf. Proc.*, vol. 2045, no. December, 2018, doi: 10.1063/1.5080833.

[16] M. N. A. Uda, U. Hashim, S. C. B. Gopinath, M. N. A. Uda, N. A. Parmin, and A. M. Isa, "Label-free aptamer based biosensor for heavy metal detection," *AIP Conf. Proc.*, vol. 2291, no. November, 2020, doi: 10.1063/5.0022834.

[17] M. N. A. Uda *et al.*, "Harumanis Mango: Perspectives in Disease Management and Advancement using Interdigitated Electrodes (IDE) Nano-Biosensor," *IOP Conf. Ser. Mater. Sci. Eng.*, vol. 864, no. 1, 2020, doi: 10.1088/1757-899X/864/1/012180.

[18] N. A. N. Yahaya, R. D. A. A. Rajapaksha, M. N. A. Uda, and U. Hashim, "Ultra-low current biosensor output detection using portable electronic reader," *AIP Conf. Proc.*, vol. 1885, 2017, doi: 10.1063/1.5002430.

[19] S. Mertin *et al.*, "Piezoelectric and structural properties of c-axis textured aluminium scandium nitride thin films up to high scandium content," *Surf. Coatings Technol.*, vol. 343, no. January, pp. 2–6, 2018, doi: 10.1016/j.surfcoat.2018.01.046.

[20] M. Soni, T. Arora, R. Khosla, P. Kumar, A. Soni, and S. K. Sharma, "Integration of Highly Sensitive Oxygenated Graphene with Aluminum Micro-Interdigitated Electrode Array Based Molecular Sensor for Detection of Aqueous Fluoride Anions," *IEEE Sens. J.*, vol. 16, no. 6, pp. 1524–1531, 2016, doi: 10.1109/JSEN.2015.2505782.

[21] R. D. A. A. Rajapaksha, N. A. N. Yahaya, M. N. A. Uda, and U. Hashim, "Development of portable electronic reader for picoampere detection for two-electrode based amperometric biosensor applications," *AIP Conf. Proc.*, vol. 2045, no. December, pp. 1–7, 2018, doi: 10.1063/1.5080834.

[22] R. D. A. A. Rajapaksha, M. N. A. Uda, U. Hashim, S. C. B. Gopinath, and C. A. N. Fernando, "Impedance based Aluminium Interdigitated Electrode (Al-IDE) biosensor on silicon substrate for salmonella detection," *IEEE Int. Conf. Semicond. Electron. Proceedings, ICSE*, vol. 2018-Augus, pp. 93–96, 2018, doi: 10.1109/SMELEC.2018.8481324.

[23] R. D. A. A. Rajapaksha, U. Hashim, N. Z. Natasha, M. N. A. Uda, V. Thivina, and C. A. N. Fernando, "Gold nano-particle based Al interdigitated electrode electrical biosensor for specific ssDNA target detection," *Proc. 2017 IEEE Reg. Symp. Micro Nanoelectron. RSM 2017*, pp. 191–194, 2017, doi: 10.1109/RSM.2017.8069167.

[24] C. Song, J. Li, J. Liu, and Q. Liu, "Simple sensitive rapid detection of Escherichia coli O157:H7 in food samples by label-free immunofluorescence strip sensor," *Talanta*, vol. 156–157, pp. 42–47, 2016, doi: 10.1016/j.talanta.2016.04.054.

[25] Y. Wu and H. Chai, "Development of an electrochemical biosensor for rapid detection of foodborne pathogenic bacteria," *Int. J. Electrochem. Sci.*, vol. 12, no. 5, pp. 4291–4300, 2017, doi: 10.20964/2017.05.09.

[26] N. A. Parmin, U. Hashim, S. C. B. Gopinath, and M. N. A. Uda, *Biosensor recognizes the receptor molecules*. Elsevier Inc., 2018.

[27] M. N. A. Uda *et al.*, "Silica and graphene mediate arsenic detection in mature rice grain by a newly patterned current–volt aptasensor," *Sci. Rep.*, vol. 11, no. 1, pp. 1–13, 2021, doi: 10.1038/s41598-021-94145-0.

[28] M. N. A. Uda *et al.*, "Immunosensor development formatting for tungro disease detection using nano-gold antibody particles application," *AIP Conf. Proc.*, vol. 1808, pp. 10–14, 2017, doi: 10.1063/1.4975290.

[29] S. C. B. Gopinath, U. Hashim, and M. N. A. Uda, "Evaluation of factor IX deficiency by interdigitated electrode (IDE)," *AIP Conf. Proc.*, vol. 1808, pp. 1–5, 2017, doi: 10.1063/1.4975250.

[30] K. Gherab *et al.*, "Fabrication and characterizations of Al nanoparticles doped ZnO nanostructures-based integrated electrochemical biosensor," *J. Mater. Res. Technol.*, vol. 9, no. 1, pp. 857–867, 2020, doi: 10.1016/j.jmrt.2019.11.025.

[31] M. N. M. N *et al.*, "Top-down nanofabrication and characterization of 20 nm silicon nanowires for biosensing applications," *PLoS One*, vol. 11, no. 3, pp. 20–23, 2016, doi: 10.1371/journal.pone.0152318.

[32] M. A. Fakhri, E. T. Salim, A. W. Abdulwahhab, U. Hashim, and Z. T. Salim, "Optical properties of micro and nano LiNbO3 thin film prepared by spin coating," *Opt. Laser Technol.*, vol. 103, pp. 226–232, 2018, doi: 10.1016/j.optlastec.2018.01.040.

[33] Y. Luo and E. C. Alocilja, "Portable nuclear magnetic resonance biosensor and assay for a highly sensitive and rapid detection of foodborne bacteria in complex matrices," *J. Biol. Eng.*, vol. 11, no. 1, pp. 1–8, 2017, doi: 10.1186/s13036-017-0053-8.

[34] N. Shoaie, M. Forouzandeh, and K. Omidfar, "Voltammetric determination of the Escherichia coli DNA using a screen-printed carbon electrode modified with polyaniline and gold nanoparticles," *Microchim. Acta*, vol. 185, no. 4, pp. 1–9, 2018, doi: 10.1007/s00604-018-2749-y.

[35] Y. Zou, J. Liang, Z. She, and H. B. Kraatz, "Gold nanoparticles-based multifunctional nanoconjugates for highly sensitive and enzyme-free detection of E.coli K12," *Talanta*, vol. 193, pp. 15–22, 2019, doi: 10.1016/j.talanta.2018.09.068.

[36] M. Zhong *et al.*, "An electrochemical immunobiosensor for ultrasensitive detection of Escherichia coli O157:H7 using CdS quantum dots-encapsulated metal-organic frameworks as signal-amplifying tags," *Biosens. Bioelectron.*, vol. 126, pp. 493–500, 2019, doi: 10.1016/j.bios.2018.11.001.

[37] Q. Guo *et al.*, "DNA-based hybridization chain reaction and biotin–streptavidin signal amplification for sensitive detection of Escherichia coli O157:H7 through ELISA," *Biosens. Bioelectron.*, vol. 86, pp. 990–995, 2016, doi: 10.1016/j.bios.2016.07.049.

[38] M. Xu, R. Wang, and Y. Li, "Electrochemical biosensors for rapid detection of Escherichia coli O157:H7," *Talanta*, vol. 162, pp. 511–522, 2017, doi: 10.1016/j.talanta.2016.10.050.